Joint Client Selection and UAV Placement in UAV-Aided Federated Learning

Seyed Soroush Tabadkani Avval, and Jingjing Yao, *Member, IEEE*
Department of Computer Science, Texas Tech University, Lubbock, TX 79409, USA.

***Abstract*—Federated Learning (FL) enables distributed clients to collaboratively train a global model without sharing raw data, offering a privacy-preserving and communication-efficient framework. Extending FL to Unmanned Aerial Vehicles (UAVs) allows UAVs to act as mobile clients that collect data from dispersed User Devices (UDs), train local models, and send updates to a ground base station for aggregation, making UAV-aided FL well-suited for infrastructure-sparse and dynamic environments. However, UAV-aided FL faces challenges due to limited UAV energy budgets, mobility constraints, and coverage limitations. In this work, we investigate the joint optimization of coverage and energy-aware client selection and UAV placement in a UAV-aided FL framework. The problem is formulated as a non-convex optimization aiming to maximize UAV participation and UD coverage under energy and mobility constraints. We propose a low-complexity algorithm based on Lyapunov optimization, combining a priority-based stochastic client selection method with a Successive Convex Approximation (SCA) approach for UAV placement. Simulation results show significant improvements in energy efficiency, UD coverage, and UAV participation compared to benchmarks.**

***Index Terms*—federated learning, client selection, UAV placement, energy efficiency, UAV mobility**

I. Introduction

Federated Learning (FL) is a decentralized machine learning paradigm that enables multiple clients to collaboratively train a shared global model without exchanging their private local data, thereby preserving data privacy and reducing communication overhead [1]. Each client computes model updates using its local dataset and transmits only the learned parameters to a central aggregator, which integrates them into a global model. In scenarios where ground infrastructure is limited, such as disaster zones, agricultural fields, or rural areas, Unmanned Aerial Vehicles (UAVs) provide a flexible and mobile platform to support FL. In UAV-aided FL framework [2]–[4], UAVs serve as clients to collect data from the ground User Devices (UDs) within their coverage area, train a local model using this data, and send the resulting parameters to a ground Base Station (BS) for aggregation.

However, the UAV-aided FL framework presents unique challenges due to UAVs' limited energy budgets, mobility constraints, and communication constraints. Client selection, determining which UAVs should participate in each global round of FL training, becomes critical in affecting both resource efficiency and learning performance [5], [6]. Activating too many UAVs risks depleting energy resources and overloading the communication network, while selecting suboptimal ones can slow convergence due to poor data quality or model staleness. Hu *et al.* [7] investigated a joint client selection and resource allocation in UAV-aided FL framework by deep reinforcement learning. Wu *et al.* [8] studied the participant and sample selection for efficient online federated learning in UAV Swarms. Tang *et al.* [9] proposed an online resource allocation algorithm to minimize the training latency by jointly deciding the selection decisions of clients and a global aggregation server. Zhao *et al.* [10] investigated the client selection and UAV scheduling problem to minimize the energy consumption. However, none of the above studies have explicitly considered the mobility of UAVs.

UAV placement problem in UAV-aided FL is also critical. Since UAVs must physically travel to UDs to collect data samples, their 3D positions affect communication latency, energy consumption, and the number of covered UDs. Inefficient placement may result in limited UD coverage or violations of energy and mobility constraints. Li *et al.* [11] jointly optimized the data collection route and UAV velocity in the UAV-aided FL framework by a two-stage combinatorial multi-armed bandit algorithm. Jing *et al.* [12] jointly optimized the UAV location and resource allocation to minimize the tradeoff between energy consumption and training latency. Zhang *et al.* [13] addressed the latency minimization problem that jointly optimizes the resource allocation and UAV trajectory to maximize training efficiency. However, none of the existing works have addressed the coverage and energy-aware joint client selection and UAV placement problem in UAV-aided FL frameworks.

In this work, we investigate the joint optimization of coverage and energy-aware client selection and UAV placement in a UAV-aided FL framework. We formulate this optimization problem to maximize the number of selected UAV clients and the number of covered UDs across all global rounds, subject to constraints on UAV energy budgets, coverage conditions, and mobility requirements. To solve this challenging non-convex problem, we propose a low-complexity algorithm based on Lyapunov optimization that decomposes the long-term objective into per-round subproblems. We then divide the per-round decision-making into two subproblems: client selection and UAV placement. The client selection subproblem is addressed using a priority-based stochastic sampling strategy, and the UAV placement subproblem is solved via the Successive Convex Approximation (SCA) method, incorporating slack-

This work was supported by the National Science Foundation under Grant No.2531678.

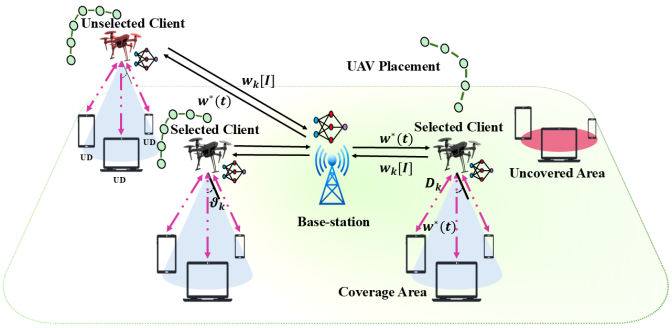

Fig. 1: System model architecture.

variable relaxation and first-order Taylor linearization. Extensive simulations validate the performance of our approach.

The remainder of this article is organized as follows. Section II introduces the system model of the UAV-aided FL framework and presents the problem formulation. Section III details the proposed algorithmic solution. Section IV provides extensive simulation results and performance analysis. Finally, Section V concludes the paper.

II. System Model

In our proposed UAV-aided FL framework (Fig. 1), K UAVs are deployed to collect data from M user devices (UDs), denoted by $\mathcal{K} = \{1, 2, \ldots, K\}$ and $\mathcal{M} = \{1, 2, \ldots, M\}$, respectively. Each UAV acts as an FL client by training a local model on the data collected from its covered UDs and then offloading the updated parameters to the base station (BS). The BS aggregates the received local models into a global model, which is broadcast back to the UAVs. This process repeats until the global model converges or a predefined number of global rounds is reached. To account for heterogeneous UAV resources, only a selected subset $\mathcal{A} \subseteq \mathcal{K}$ participates in aggregation during each round.

A. Latency Model

In our system, the total latency of UAV k in each global round consists of three components: the computation latency for local model training, the communication latency for uploading the local model to the ground BS, and the flight latency required for UAV mobility [14]. The computation latency of UAV k is expressed as

$$T_k^{\text{cmp}} = L_k \frac{C_k D_k}{f_k}, \tag{1}$$

where L_k is the number of local iterations, C_k denotes the required CPU cycles per data sample, D_k is the local dataset size, and f_k represents the CPU frequency (in cycles per second) [3].

To characterize the wireless communication channel between each UAV k and the ground BS, we adopt a probabilistic air-to-ground path loss model that accounts for both line-of-sight (LoS) and non-line-of-sight (NLoS) propagation conditions [15]. The large-scale path loss g_k is modeled as a combination of free-space path loss and additional attenuation weighted by the probabilities of LoS and NLoS links $g_k = PL_k + \eta_{\text{LoS}} P_k^{\text{LoS}} + \eta_{\text{NLoS}}(1 - P_k^{\text{LoS}})$, where $PL_k = 10 \log_{10} \left(\frac{4\pi f_c d_k}{c} \right)^{\beta}$ represents the free-space path loss, with f_c denoting the carrier frequency, c the speed of light, β the path loss exponent, and d_k the distance between UAV k and the BS. The LoS probability P_k^{LoS} is expressed as a function of the elevation angle θ using $P_k^{\text{LoS}} = \frac{1}{1 + a \exp(-b[\arctan(\theta) - a])}$, where a and b are constants determined by the propagation environment (e.g., urban or rural). Small-scale fading is modeled by a complex Gaussian random variable $\bar{h}_k \sim \mathcal{CN}(0, 1)$, and the overall channel gain is given as $h_k = \sqrt{g_k} \bar{h}_k$. Based on this channel model, the uplink transmission rate between UAV k and the BS is obtained from the Shannon capacity $r_k = b_k \log_2 \left(1 + \frac{p_k |h_k|^2}{N_0} \right)$, where b_k is the bandwidth allocated to UAV k, p_k denotes the UAV's transmit power, and N_0 is the noise power spectral density. where b_k is the bandwidth allocated to UAV k, p_k its transmit power, and N_0 the noise power spectral density. Finally, the communication latency for UAV k to offload its local model of size s_k to the BS is

$$T_k^{\text{com}} = \frac{s_k}{r_k}. \tag{2}$$

We optimize UAV flight locations in each global round and assume that UAVs move along straight-line trajectories between successive positions with a fixed speed V_k. The 3D location of UAV k at global round t is defined as $l_k(t) = \langle x_k(t), y_k(t), z_k(t) \rangle$. Accordingly, the flight time of UAV k at round t is computed as

$$T_k^{\text{mov}}(t) = \frac{\| l_k(t+1) - l_k(t) \|_2}{V_k}, \tag{3}$$

where $\| \cdot \|$ is the Euclidean distance operator. Combining all components, the total latency of UAV k in global round t, including computation, communication, and mobility, is

$$T_k^{\text{total}}(t) = T_k^{\text{cmp}}(t) + T_k^{\text{com}}(t) + T_k^{\text{mov}}(t). \tag{4}$$

B. Energy Model

The energy consumption of each UAV k in a global round consists of three components: local computation, wireless communication, and propulsion for mobility. The computation energy for performing L_k local iterations follows the dynamic power model [3]:

$$E_k^{\text{cmp}} = L_k \alpha_k C_k D_k f_k^2, \tag{5}$$

where α_k is the effective switched capacitance of the processor. The energy consumption for data transmission is

$$E_k^{\text{com}} = p_k T_k^{\text{com}}. \tag{6}$$

The propulsion power required for UAV mobility is modeled as [16]

$$p_k^{\text{prop}}(t) = U_1 \left(1 + \frac{3 \text{v}_k^2(t)}{\text{v}_{\text{tip}}^2} \right) + U_2 \sqrt{\left(U_3 + \frac{\text{v}_k^4(t)}{4} - \frac{\text{v}_k^2(t)}{2} \right)} + U_4 \text{v}_k^3(t) + W \text{v}_k^z(t), \tag{7}$$

where U_1, U_2, U_3, U_4 are constants related to UAV weight and aerodynamics, v_{tip} is the rotor tip speed, W is the UAV weight, $\mathrm{v}_k(t) = \frac{\|\langle x_k(t+1)-x_k(t), y_k(t+1)-y_k(t)\|_2}{T_k^{\text{mov}}(t)}$ is the horizontal speed, and $\mathrm{v}_k^z(t) = \frac{z_k(t+1)-z_k(t)}{T_k^{\text{mov}}(t)}$ is the vertical speed. The propulsion energy is then

$$E_k^{\text{prop}}(t) = p_k^{\text{prop}}(t) T_k^{\text{mov}}(t). \tag{8}$$

Finally, the total energy consumption of UAV k in global round t is

$$E_k^{\text{total}}(t) = E_k^{\text{cmp}}(t) + E_k^{\text{com}}(t) + E_k^{\text{prop}}(t). \tag{9}$$

C. UAV Coverage

In our system, each UAV k provides a 2D circular coverage area on the ground, centered at its projected position $\langle x_k, y_k \rangle$. The coverage radius is defined as $R_k = z_k \tan(\vartheta_k)$, where ϑ_k is the antenna's half-beamwidth angle [17]. A UD m located at $\langle x_m, y_m \rangle$ is considered covered if its Euclidean distance to the UAV's projection $d_{mk} = \|\langle x_m - x_k, y_m - y_k \rangle\|_2$ satisfies $d_{mk} \leq R_k$. The total number of UDs covered by UAV k in round t is given by $N_k(t) = \sum_{m \in \mathcal{M}} I_{mk}(t)$, where the indicator function $I_{mk}(t) = 1$ if UD m is covered and $I_{mk}(t) = 0$ otherwise.

D. Problem Formulation

The joint coverage and energy-aware optimization of FL client selection and UAV placement in a UAV-aided FL framework is formulated as problem $\mathcal{P}_0$:

$$\mathcal{P}_0 : \max_{\rho_k, x_k, y_k, z_k} \left(\sum_{t \in \mathcal{T}} \sum_{k \in \mathcal{K}} \rho_k(t) + \sum_{t \in \mathcal{T}} \sum_{k \in \mathcal{K}} \rho_k(t) N_k(t) \right)$$

$$\text{s.t.} \sum_{t \in \mathcal{T}} \rho_k(t) E_k^{total}(t) \leq \mathcal{J}_k, \ \forall k \in \mathcal{K}, \tag{C1}$$

$$N_k(t) = \sum_m I_{mk}(t), \ \forall k \in \mathcal{K}, t \in \mathcal{T}, \tag{C2}$$

$$I_{mk}(t) = \begin{cases} 1, & \text{if } d_{mk}(t) \leq R_k(t), \\ 0, & \text{otherwise}, \end{cases} \quad \forall k \in \mathcal{K}, \forall m \in \mathcal{M}, t \in \mathcal{T}, \tag{C3}$$

$$x_k(0) = x_k(T), \ y_k(0) = y_k(T), z_k(0) = z_k(T), \quad \forall k \in \mathcal{K}, t \in \mathcal{T}, \tag{C4}$$

$$0 \leq x_k(t) \leq X^{max}, \ \forall k \in \mathcal{K}, t \in \mathcal{T}, \tag{C5}$$

$$0 \leq y_k(t) \leq y^{max}, \ \forall k \in \mathcal{K}, t \in \mathcal{T}, \tag{C6}$$

$$Z^{min} \leq z_k(t) \leq Z^{max}, \ \forall k \in \mathcal{K}, t \in \mathcal{T}, \tag{C7}$$

$$\rho_k(t) \in \{0, 1\}, \ \forall k \in \mathcal{K}, t \in \mathcal{T}. \tag{C8}$$

The objective maximizes both the number of selected UAV clients and the number of covered UDs over T global rounds, where $\rho_k(t)$ indicates whether UAV k is selected in round t. Constraint (C1) enforces the energy budget $\mathcal{J}_k$ for each UAV. Constraints (C2)–(C3) determine UD coverage. Constraint (C4) ensures UAVs return to their starting positions. Constraints (C5)–(C7) confine UAV positions to a bounded 3D operational space, while (C8) imposes binary selection.

Problem $\mathcal{P}_0$ is non-convex due to the binary variables, nonlinear coverage conditions, and discontinuous constraints, making it computationally challenging to solve directly. Therefore, in the next section, we design a low-complexity algorithm to efficiently obtain its solution.

III. Algorithm Design

In this section, we present a low-complexity algorithm to solve the joint client selection and UAV placement problem in the UAV-aided FL framework. The key idea is to leverage the Lyapunov drift-plus-penalty framework to decompose the original long-term optimization into a sequence of independent per-round subproblems. Within each round, the problem is further divided into two subproblems: client selection and UAV placement. The client selection subproblem is solved using a priority-based heuristic with stochastic sampling, which preferentially selects UAVs with stale models and larger datasets. The UAV placement subproblem is tackled using the SCA method, where slack-variable relaxation and first-order Taylor expansions transform the original non-convex formulation into a sequence of convex subproblems that can be efficiently solved.

We leverage the Lyapunov optimization framework to incorporate the long-term energy constraint, which is well-suited for handling time-averaged constraints in dynamic systems. The energy constraint (C1) requires that the cumulative energy consumption of each UAV across T global rounds remain within its finite energy budget $\mathcal{J}_k$. Directly enforcing this condition, however, introduces temporal coupling among decisions across rounds, making the problem non-convex and computationally intractable.

To address this challenge, we introduce a virtual queue mechanism that converts the long-term energy constraint into a queue stability problem. For each UAV k, we define a virtual energy queue $Q_k(t)$ that records the accumulated deviation from its ideal average energy budget $\frac{\mathcal{J}_k}{T}$ per round. The queue evolves according to $Q_k(t+1) = \max\left\{Q_k(t) + \rho_k(t) E_k^{\text{total}}(t) - \frac{\mathcal{J}_k}{T}, \ 0\right\}$, where $\rho_k(t) E_k^{\text{total}}(t)$ represents the actual energy consumed in global round t. If UAV k consumes more than its per-round share of the budget, the queue grows. Otherwise, if it consumes less, the queue decreases or remains stable. By ensuring the stability of these virtual queues, we indirectly guarantee that the cumulative long-term energy constraint is satisfied.

The Lyapunov optimization framework reformulates the problem into a per-round decision-making process that jointly balances the system objective in $\mathcal{P}_0$ and the stability of the virtual energy queues. We define the Lyapunov function as $L(t) = \frac{1}{2} \sum_k Q_k^2(t)$, which captures the aggregate energy pressure in the system. The corresponding Lyapunov drift is $\Delta(t) = L(t+1) - L(t)$ whose upper bound can be expressed as $\Delta(t) \leq \sum_k Q_k(t) \left(\rho_k(t) E_k^{\text{total}}(t) - \frac{\mathcal{J}_k}{T}\right)$. We minimize the drift-plus-penalty expression, where a control parameter

$V > 0$ weights the importance of the original objective relative to energy stability. The resulting per-round problem $\mathcal{P}_1$ is

$$\mathcal{P}_1 : \min_{\rho_k, x_k, y_k, z_k} \sum_{k\in\mathcal{K}} Q_k(t) E_k^{\text{total}}(t)\rho_k(t) - V\left[\sum_{k\in\mathcal{K}} \rho_k(t) + \sum_{k\in\mathcal{K}} \rho_k(t) N_k(t)\right]$$
$$\text{s.t. (C2)} - \text{(C8)}.$$

This formulation decouples the long-term optimization into independent per-round subproblems that rely only on current system information, while implicitly ensuring the satisfaction of long-term energy constraints. It can be further decomposed into a client selection subproblem $\mathcal{P}_2$ and a UAV placement subproblem $\mathcal{P}_3$. The client selection subproblem $\mathcal{P}_2$ can be formulated as

$$\mathcal{P}_2 : \min_{\rho_k} \sum_{k\in\mathcal{K}} Q_k(t) E_k^{\text{total}}(t)\rho_k(t) - V\left[\sum_{k\in\mathcal{K}} \rho_k(t) + \sum_{k\in\mathcal{K}} \rho_k(t) N_k(t)\right]$$
$$\text{s.t. (C8)}.$$

The UAV placement subproblem $\mathcal{P}_3$ can be formulated as

$$\mathcal{P}_3 : \min_{x_k, y_k, z_k} \sum_{k\in\mathcal{K}} Q_k(t) E_k^{\text{total}}(t)\rho_k(t) - V\sum_{k\in\mathcal{K}} \rho_k(t) N_k(t)$$
$$\text{s.t. (C2)} - \text{(C7)}.$$

Algorithm 1 Client Selection

Input: t, $\rho_k(t-1)$, D_k, χ, $\mathcal{K}$, $\mathcal{A}$.
Initiliaze $\rho_k(t) \leftarrow 0$, for all k
for each UAV $k \in \mathcal{K}$ **do**
  if $\rho_k(t-1) = 0$ **then**
    $A_k(t) \leftarrow A_k(t-1) + 1$
  else
    $A_k(t) \leftarrow 1$
  end if
  $\pi_k^{\text{prior}}(t) \leftarrow \frac{A_k(t)}{\sum_{k'\in\mathcal{K}} A_{k'}(t)} D_k$
  $\pi_k^{\text{temp}}(t) \leftarrow \left(\pi_k^{\text{prior}}(t)\right)^{1/\chi}$
  $w_k(t) \leftarrow \frac{\pi_k^{\text{temp}}(t)}{\sum_{k'\in\mathcal{K}} \left(\pi_{k'}^{\text{prior}}(t)\right)^{1/\chi}}$
end for
$\mathcal{A}(t) \leftarrow \text{Sample}(\mathcal{A}, \{w_k(t)\})$
for each $k \in \mathcal{A}(t)$ **do**
  $\rho_k(t) \leftarrow 1$
end for
Output: $\mathcal{A}(t)$, $\rho_k(t)$.

To address the client selection subproblem $\mathcal{P}_2$, we design a priority-based heuristic with stochastic sampling that balances exploitation of high-priority UAVs and exploration of others. Each UAV k maintains an age variable $A_k(t)$, representing how many rounds have passed since its last participation. If $\rho_k(t) = 0$, then $A_k(t) = A_k(t-1) + 1$, while if $\rho_k(t) = 1$, the age is reset to $A_k(t) = 1$. This mechanism ensures UAVs with stale models accumulate higher priority over time. We define the priority weight as $\pi_k^{\text{prior}}(t) = a_k(t) D_k$, where D_k is the dataset size of UAV k, and $a_k(t) = \frac{A_k(t)}{\sum_{j\in\mathcal{K}} A_j(t)}$ is the normalized age. Thus, UAVs with both large datasets and outdated models receive higher priority. To prevent deterministic selection, we adopt a stochastic scheme based on a softmax-like distribution $w_k(t) = \frac{\left(\pi_k^{\text{prior}}(t)\right)^{1/\chi}}{\sum_{j\in\mathcal{K}} \left(\pi_j^{\text{prior}}(t)\right)^{1/\chi}}$, where $\chi > 0$ is a temperature parameter. A small χ favors deterministic selection of high-priority UAVs, while a larger χ increases randomness, encouraging exploration [18]. UAVs are then sampled according to $w_k(t)$ to form the set of selected clients in round t. The client selection algorithm is summarized in Algorithm 1.

Algorithm 2 UAV Placement

Input: t, $l_k^0(t)$, $\mathcal{K}$, $maxS$, T.
Initialize $l_k^0(t) = (x_k^0(t), y_k^0(t), z_k^0(t))$, $\xi_{mk}(t) \leftarrow 0$
if $t = T$ **then**
  set $l_k(t) \leftarrow l_k(0)$ for all k
end if
for each iteration $s = 1$ to $maxS$ **do**
  Solve the convex subproblem $\mathcal{P}_4$ using linearizations around $l_k^{s-1}(t)$
  Obtain updated positions $l_k^s(t)$
  if $\|l_k^s(t) - l_k^{s-1}(t)\| < 10^{-3}$ for all k **then**
    break
  end if
end for
$l_k(t) \leftarrow l_k^s(t)$ for all k
Output: $l_k(t)$.

For the UAV placement subproblem $\mathcal{P}_3$, the main challenge is the non-convexity introduced by binary coverage indicators and nonlinear propulsion energy terms. To address this challenge, we employ the SCA method, which iteratively solves convex approximations of the original problem until convergence. The coverage constraint $d_{mk}(t) \le z_k(t)\tan(\vartheta_k)$ is first relaxed by introducing non-negative slack variables $\xi_{mk}(t)$, namely, $d_{mk}(t) \le z_k(t)\tan(\vartheta_k) + \xi_{mk}(t)$. Then, the binary indicator $I_{mk}(t)$ is approximated by a continuous surrogate $I_{mk}(t) \approx 1 - \frac{\xi_{mk}(t)}{z_k(t)\tan(\vartheta_k)}$, and the total number of covered UDs for UAV k becomes $N_k(t) \approx M - \frac{1}{z_k(t)\tan(\vartheta_k)} \sum_{m\in\mathcal{M}} \xi_{mk}(t)$. To discourage excessive violations, a penalty term $\eta \sum_m \sum_k \xi_{mk}(t)$ is added to the objective function, which forces the slack variables toward zero and thereby encourages the UAVs to satisfy the original coverage condition. Moreover, we linearize the non-linear terms based on the first-order Taylor expansion. Specifically, the distance d_{mk}, the coverage $N_k(t)$, and the total energy consumption E_k^{total} is approximated by $\tilde{d}_{mk}^s(t)$, $\tilde{N}_k^s(t)$, and $\tilde{E}_k^{\text{total},s}$ respectively around the current location l_k^{s-1}, where s is the number of iterations. Putting all these approximations

together, the approximate convex subproblem of problem $\mathcal{P}_3$ is given by

$$\mathcal{P}_4: \min_{x_k,y_k,z_k,\xi_{mk}} \sum_k Q_k(t)\tilde{E}_k^{\text{total},s}(t) - V\sum_k \tilde{N}_k^s(t) + \eta\sum_k\sum_m \xi_{mk}(t)$$
$$\text{s.t.} \quad \tilde{d}_{mk}^s(t) \le z_k(t)\tan(\vartheta_k) + \xi_{mk}(t), \ \forall m,k,$$
$$\xi_{mk}(t) \ge 0, \ \forall m,k,$$
$$\text{(C2)}, \text{(C4)} - \text{(C7)}.$$

The solution $l_k^s(t)$ of this convex problem can be obtained by optimization solvers like CPLEX [19]. The updated solution $l_k^s(t)$ is used as the new expansion point for the first-order Taylor approximation in the next iteration. The process continues until convergence $\|l_k^s(t) - l_k^{s-1}(t)\| < \epsilon$ or a maximum number of iterations is reached. Finally, to ensure that UAVs return to their initial positions by the final round $t = T$, we set $l_k(T) = l_k(0)$. The UAV placement algorithm is detailed in Algorithm 2.

IV. Simulation Results

In this section, we evaluate the performance of our proposed (denoted as Proposed) algorithm. The experiments were conducted on a Dell workstation with an Intel Xeon W-2245 (3.90GHz, 16 cores), NVIDIA Quadro RTX 6000/8000 GPU, and 128GB RAM. We compare our proposed algorithm with three benchmark algorithms MADDPG, Greedy, and Fixed. MADDPG, inspired by [20], employs a multi-agent deep deterministic policy gradient framework to optimize UAV trajectories and client selection. Greedy, inspired by [21], is a heuristic method that selects clients by prioritizing UDs with the largest local datasets and positions UAVs by iteratively placing them at the centroid of the selected clients' locations. Fixed, inspired by [22], uses uniform client selection, where UDs are selected with equal probability, and fixed UAV trajectories (circular) without adaptive optimization.

The simulation involved $K = 5$ UAVs and $M = 50$ UDs randomly distributed in a $500 \times 500\,m^2$ area. UAV coverage radius R_k depends on altitudes (uniformly distributed in $[50, 100]\,m$) and antenna angle $\vartheta_k = 45°$. The LoS probability uses environment constants $a = 9.61$ and $b = 0.25$, with LoS and NLoS attenuations $\eta_{\text{LoS}} = 1\,\text{dB}$ and $\eta_{\text{NLoS}} = 20\,dB$. Bandwidth per UAV is $10\,MHz$, with noise power $N_0 = -174\,dBm/Hz$ and channel gain $\beta = -50\,dB$ at $1\ m$. Transmission powers range from $[0.1, 1.0]\,W$. The simulation ran for $T = 100$ global rounds with $L_k = 1$ local iteration, UAV energy budget $\mathcal{J}_k = 100\,J$, effective capacitance $\alpha_k = 10^{-28}$, CPU frequency f_k range from $[1, 10]\,GHz$, CPU cycles per sample $C_k = 10^3$, UAV speed $V_k = 10\,m/s$. UAV propulsion constants are $U_1 = 0.1\,W, U_2 = 1000\,W, U_3 = 500\,W, U_4 = 0.01\,W/(m/s)^3$, rotor tip speed $v_{\text{tip}} = 120\,m/s$, and UAV weight $W = 5\,kg$. The FL setup uses a Convolutional Neural Network (CNN) trained on the MNIST dataset distributed in a Non-IID distribution. Each UD contributes 100–500 samples of $D_k = 0.01\ MB$, and UAVs contribute a model size of $s_k = 0.2\ MB$, and client selection uses an exploration-exploitation parameter of $\chi = 1.5$.

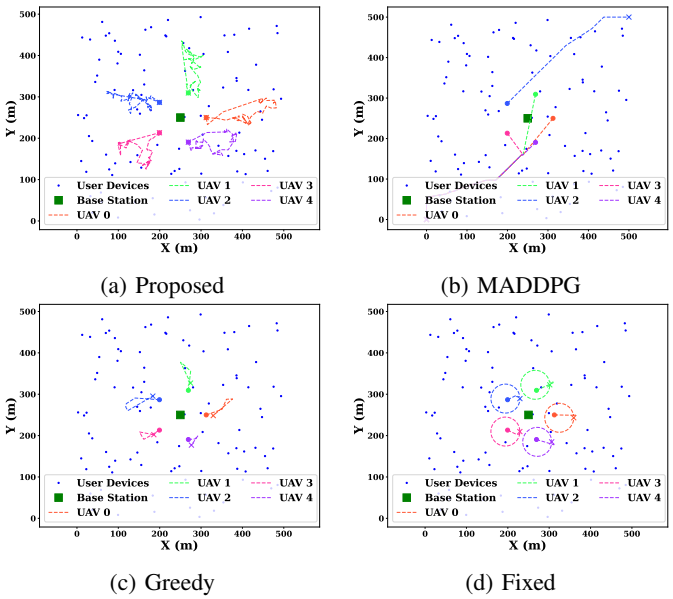

(a) Proposed (b) MADDPG

(c) Greedy (d) Fixed

Fig. 2: Performance on UAV placement.

Fig. 2 illustrates the UAV placements under four different algorithms. We can observe that the Proposed algorithm adaptively distributes UAVs to cover dense clusters of user devices, which results in both wide and balanced coverage. In contrast, MADDPG places UAVs unevenly, with some flying far away and wasting energy. Greedy often traps UAVs in locally optimal regions, missing broader coverage opportunities, and Fixed keeps UAVs fixed in symmetric positions, leaving many devices uncovered. These comparisons demonstrate that the Proposed algorithm achieves the best coverage performance.

Fig. 3 shows the average number of selected UAV clients per round as the number of users increases under different algorithms. We can observe that the Proposed algorithm consistently selects the maximum number of UAVs as the number of users grows, ensuring higher client participation and better utilization of available resources. In contrast, MADDPG exhibits lower client participation, particularly at higher user counts, indicating limited adaptability to larger user populations. Greedy shows moderate performance but struggles to maintain consistent client engagement as the number of users increases. Fixed, employing a uniform random selection strategy, results in stable but suboptimal client participation, failing to optimize for coverage or resource efficiency.

Fig. 4 illustrates the energy consumption of different algorithms as the number of UAVs increases. We can observe that Proposed consistently achieves the lowest energy cost and grows only slightly with more UAVs, showing that it effectively manages propulsion and communication overhead. In contrast, both Greedy and MADDPG incur rapidly increasing energy consumption as the UAV count rises, with Greedy performing the worst due to myopic placement decisions that

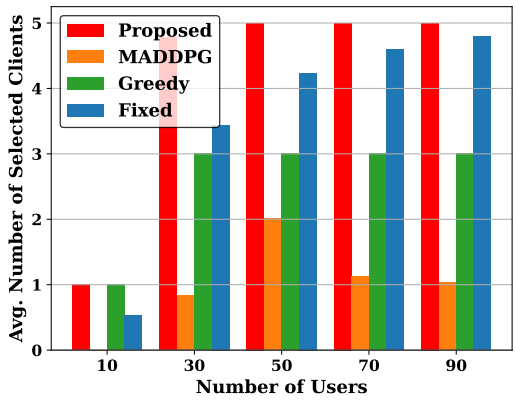

Fig. 3: Performance on client selection.

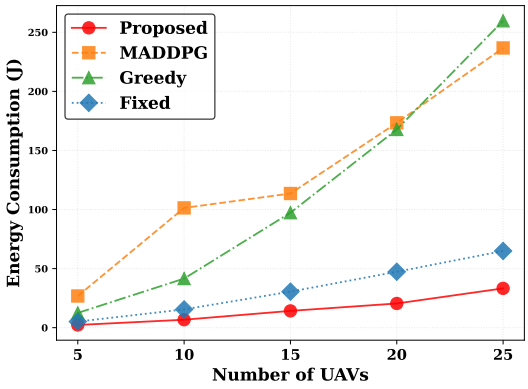

Fig. 4: Energy consumption vs number of UAVs.

waste energy. Fixed consumes more energy than the Proposed method but remains lower than Greedy and MADDPG, as its fixed symmetric placement avoids extreme inefficiencies but ignores device distribution.

V. Conclusion

In this work, we have investigated the problem of coverage and energy-aware client selection and UAV placement in a UAV-aided FL framework. We have formulated a joint optimization problem that maximizes UAV participation and user device coverage under energy, mobility, and coverage constraints. To address the non-convexity and long-term coupling in the optimization, we have designed a low-complexity algorithm based on Lyapunov optimization, which decomposes the original problem into per-round client selection and UAV placement subproblems. The client selection is solved using a priority-based stochastic sampling strategy, while the UAV placement is addressed using a SCA approach. Extensive simulation results have demonstrated that our proposed algorithm significantly improves the performance on energy efficiency, client participation, and user coverage compared to benchmark approaches.

References

[1] J. Yao and N. Ansari, "Enhancing federated learning in fog-aided IoT by CPU frequency and wireless power control," *IEEE Internet Things J.*, vol. 8, no. 5, pp. 3438–3445, 2021.

[2] S. Cal, X. Sun, and J. Yao, "Energy-efficient federated knowledge distillation learning in internet of drones," in *2024 IEEE Int. Conf. Commun. Workshops (ICC Workshops)*, 2024, pp. 1256–1261.

[3] J. Yao, S. Cal, and X. Sun, "Resource allocation for federated knowledge distillation learning in internet of drones," *IEEE Internet Things J.*, vol. 12, no. 7, 2025.

[4] J. Yao and N. Ansari, "Secure federated learning by power control for internet of drones," *IEEE Trans. Cogn. Commun. Netw.*, vol. 7, no. 4, pp. 1021–1031, 2021.

[5] R. Albelaihi *et al.*, "Deep-reinforcement-learning-assisted client selection in nonorthogonal-multiple-access-based federated learning," *IEEE Internet Things J.*, vol. 10, no. 17, pp. 15 515–15 525, 2023.

[6] S. Cal, X. Sun, and J. Yao, "Client selection in fault-tolerant federated reinforcement learning for IoT networks," in *ICC 2024 - IEEE Int. Conf. Commun.*, 2024, pp. 459–464.

[7] W. Hu *et al.*, "Multi-job hierarchical federated learning for consumer-grade UAVs: A joint client selection and resource allocation approach," *IEEE Trans. Consum. Electron.*, pp. 1–1, 2025.

[8] F. Wu *et al.*, "Participant and sample selection for efficient online federated learning in UAV swarms," *IEEE Internet Things J.*, vol. 11, no. 12, pp. 21 202–21 214, 2024.

[9] J. Tang *et al.*, "Multi-UAV-assisted federated learning for energy-aware distributed edge training," *IEEE Trans. Netw. Serv. Manag.*, vol. 21, no. 1, pp. 280–294, 2024.

[10] H. Zhao *et al.*, "Safe and saving: A joint learning and energy-efficient scheduling scheme of UAV assisted hierarchical federated learning for remote inspection within large scale iiot," *IEEE Internet Things J.*, vol. 12, no. 13, pp. 25 357–25 370, 2025.

[11] D. Li *et al.*, "Optimizing data-driven federated learning in UAV networks," in *2024 IEEE 30th Int. Conf. Parallel Distrib. Syst. (ICPADS)*, 2024, pp. 9–17.

[12] Y. Jing *et al.*, "Exploiting UAV for air-ground integrated federated learning: A joint UAV location and resource optimization approach," *IEEE Trans. Green Commun. Netw.*, vol. 7, no. 3, pp. 1420–1433, 2023.

[13] X. Zhang *et al.*, "Latency minimization for UAV-enabled federated learning: Trajectory design and resource allocation," *IEEE Internet Things J.*, vol. 12, no. 14, pp. 27 097–27 112, 2025.

[14] Q.-V. Pham *et al.*, "Energy-efficient federated learning over uav-enabled wireless powered communications," *IEEE Trans. Veh. Technol.*, vol. 71, no. 5, pp. 4977–4990, 2022.

[15] Y. Li *et al.*, "Multiagent uav-aided urllc mobile edge computing systems: A joint communication and computation optimization approach," *IEEE Syst. J.*, 2024.

[16] X.-H. Lin *et al.*, "A lyapunov-based approach to joint optimization of resource allocation and 3-d trajectory for solar-powered uav mec systems," *IEEE Internet Things J.*, vol. 11, no. 11, pp. 20 797–20 815, 2024.

[17] Y. Shen *et al.*, "Joint training and resource allocation optimization for federated learning in uav swarm," *IEEE Internet Things J.*, vol. 10, no. 3, pp. 2272–2284, 2022.

[18] B. Wu, F. Fang, and X. Wang, "Joint age-based client selection and resource allocation for communication-efficient federated learning over noma networks," *IEEE Trans. Commun.*, vol. 72, no. 1, pp. 179–192, 2023.

[19] S. Nickel *et al.*, "Decision optimization with ibm ilog cplex optimization studio," *Angew. Optimierung IBM ILOG CPLEX Optim. Studio, Springer, Berlin/Heidelberg, Germany*, 2022.

[20] X. Fan *et al.*, "Uav-enabled federated learning in dynamic environments: Efficiency and security trade-off," *IEEE Trans. Veh. Technol.*, vol. 73, no. 5, pp. 6993–7006, 2023.

[21] R. Khelf, E. Driouch, and W. Ajib, "On the optimization of uav-assisted wireless networks for hierarchical federated learning," in *2023 IEEE 34th Ann. Int. Symp. Pers., Indoor Mobile Radio Commun. (PIMRC)*. IEEE, 2023, pp. 1–6.

[22] M. Fu, Y. Shi, and Y. Zhou, "Federated learning via unmanned aerial vehicle," *IEEE Trans. Wireless Commun.*, vol. 23, no. 4, pp. 2884–2900, 2023.